

# Optical Phonon Lasing in Semiconductor Double Quantum Dots

Rin Okuyama,<sup>1,\*</sup> Mikio Eto,<sup>1</sup> and Tobias Brandes<sup>2</sup>

<sup>1</sup>Faculty of Science and Technology, Keio University, Yokohama 223-8522, Japan

<sup>2</sup>Institut für Theoretische Physik, Technische Universität Berlin, D-10623 Berlin, Germany

(Dated: December 3, 2024)

We propose optical phonon lasing for a semiconductor double quantum dot weakly coupled to two LO phonon modes that act as a natural cavity. Lasing occurs for pumping the dot via electronic tunneling at rates much larger than the phonon decay rate, whereas anti-bunching of phonon emission is observed in the opposite regime of very slow tunneling. Both effects disappear by a Franck-Condon induced effective thermalization for strong electron-phonon coupling.

PACS numbers: 73.21.La,71.38.-k,42.50.Pq

Electrically tunable two-level systems are ideal candidates to study the interaction between fermions and bosons under nonequilibrium conditions. Single-qubit lasers or nanomechanical resonators [1–3] are examples where concepts from quantum optics, such as the micro-laser [4], have been successfully transferred to and combined with artificial solid-state architectures. Semiconductor double quantum dots (DQDs) play a similar role as model systems with the coupling between electrons and the surrounding substrate leading to, e.g., tunable spontaneous phonon emission and Dicke-type interference effects [5–7].

In this Letter, we propose optical phonon lasing in a DQD without the requirement of an additional cavity or resonator. We start from the observation that a DQD effectively couples to only two LO phonon modes which work as a natural cavity, cf. Fig. 1(b). The pumping to the upper level is then realized by an electric current through the DQD under a finite bias. The amplified LO phonons occasionally escape from this natural cavity and turn into so-called “daughter phonons” [8] that can be observed externally.

The phonon lasing discussed here is a weak-coupling effect [9] that is spoilt by phonon thermalization via the Franck-Condon effect [10–12] for strong electron-phonon coupling. We provide analytical results for the lasing at strong pumping and the  $n$ -phonon resonances as made visible in the current, phonon number, and phonon autocorrelation function  $g^{(2)}$ .

The  $g^{(2)}$ -function also quantifies a crossover to phonon anti-bunching at strong phonon decay. This is due to the strong correlation between the electron transport and the phonon lasing dynamics which is consistent with a similar observation for DQDs coupled to photons [13]. We mention that LO-phonon-assisted transport through a DQD was theoretically studied in Ref. [14] and recently observed by Amaha and Ono [15].

Figure 1(a) shows our model of a DQD in which two single energy level quantum dots  $L$  and  $R$  are connected by a tunnel coupling  $V_C$ . The level spacing  $\Delta$  between the dots is assumed to be tunable, and the total number of electrons in the DQD is restricted to one or zero by the

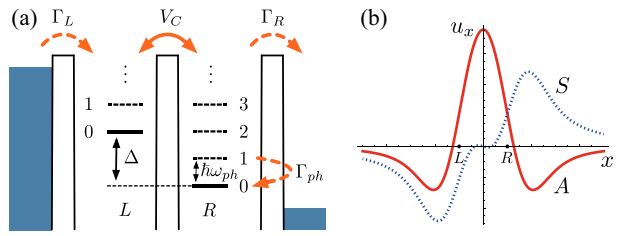


FIG. 1. (color online). (a) Model for a double quantum dot (DQD) coupled to LO phonons. A large bias is applied between external leads. The spacing  $\Delta$  between the energy levels in dots  $L$  and  $R$  is electrically tunable. When  $\Delta$  matches an integer ( $\nu$ ) multiple of the phonon energy  $\hbar\omega_{\text{ph}}$ , the electronic state  $|L\rangle$  with  $n$  phonons is coherently coupled to  $|R\rangle$  with  $(n+\nu)$  phonons. (b) The phonon mode functions  $\mathbf{u}(\mathbf{r})$  along a line through the centers of quantum dots located at  $x = \pm R$ , when the wavefunctions  $|L\rangle$  and  $|R\rangle$  are spherical with radius  $R$ . The  $x$ -component of  $\mathbf{u}(x, 0, 0)$  is shown for  $S(A)$ -phonons which couple (anti-)symmetrically to the DQD.

Coulomb blockade. The electron couples to dispersionless LO phonons of energy  $\hbar\omega_{\text{ph}}$  via the Fröhlich interaction. Our system Hamiltonian  $\mathcal{H} = \mathcal{H}_{\text{e}} + \mathcal{H}_{\text{ph}} + \mathcal{H}_{\text{ep}}$  is

$$\mathcal{H}_{\text{e}} = \frac{\Delta}{2}(n_L - n_R) + V_C(d_L^\dagger d_R + d_R^\dagger d_L), \quad (1)$$

$$\mathcal{H}_{\text{ph}} = \hbar\omega_{\text{ph}} \sum_{\mathbf{q}} N_{\mathbf{q}}, \quad \mathcal{H}_{\text{ep}} = \sum_{\alpha=L,R; \mathbf{q}} M_{\alpha, \mathbf{q}} (a_{-\mathbf{q}} + a_{\mathbf{q}}^\dagger) n_{\alpha},$$

using creation (annihilation) operators  $d_{\alpha}^\dagger$  ( $d_{\alpha}$ ) for an electron in dot  $\alpha$  and  $a_{\mathbf{q}}^\dagger$  ( $a_{\mathbf{q}}$ ) for a phonon with wave vector  $\mathbf{q}$ .  $n_{\alpha} = d_{\alpha}^\dagger d_{\alpha}$  and  $N_{\mathbf{q}} = a_{\mathbf{q}}^\dagger a_{\mathbf{q}}$  are the number operators. The spin index is omitted for electrons. The coupling constant is given by  $M_{\alpha, \mathbf{q}} = \sqrt{\frac{e^2 \hbar \omega_{\text{ph}}}{V}} \left( \frac{1}{\epsilon(\infty)} - \frac{1}{\epsilon(0)} \right) \frac{1}{q} \langle \alpha | e^{-i\mathbf{q} \cdot \mathbf{r}} | \alpha \rangle$ , where  $|\alpha\rangle$  is the electron wavefunction in dot  $\alpha$ ,  $\epsilon(\infty)$  [ $\epsilon(0)$ ] is the dielectric constant at high [low] frequency, and  $V$  is the volume of substrate. The LO phonons only around the  $\Gamma$  point ( $|\mathbf{q}| \lesssim 1/R$  with dot radius  $R$ ) are coupled to the DQD because of an oscillating factor in  $M_{\alpha, \mathbf{q}}$ . We assume equivalent quantum dots  $L$  and  $R$ , whence  $M_{R, \mathbf{q}} = M_{L, \mathbf{q}} e^{-i\mathbf{q} \cdot \mathbf{r}_{LR}}$  with  $\mathbf{r}_{LR}$  being a vector joining

their centers.

In  $\mathcal{H}_{\text{ep}}$ , we can introduce collective phonon coordinates

$$a_{S(A)}^\dagger \equiv C_{S(A)}(a_L^\dagger \pm a_R^\dagger), \quad a_\alpha^\dagger \equiv \frac{\sum_{\mathbf{q}} M_{\alpha,\mathbf{q}} a_{\mathbf{q}}^\dagger}{(\sum_{\mathbf{q}} |M_{\alpha,\mathbf{q}}|^2)^{1/2}} \quad (2)$$

and other modes orthogonal to  $a_S^\dagger$  and  $a_A^\dagger$ , where  $C_{S(A)} = 1/\sqrt{2(1 \pm \mathcal{S})}$  with the overlap integral  $\mathcal{S}$  between  $a_L^\dagger$  and  $a_R^\dagger$  phonons. Disregarding the modes decoupled from the DQD, we thus obtain the effective Hamiltonian  $H = \mathcal{H}_e + \mathcal{H}'$  where

$$\mathcal{H}' \equiv \hbar\omega_{\text{ph}} \sum_{\sigma=S,A} [N_\sigma + \lambda_\sigma(a_\sigma + a_\sigma^\dagger)(n_L \pm n_R)], \quad (3)$$

with the number operators  $N_\sigma \equiv a_\sigma^\dagger a_\sigma$ , the couplings  $\lambda_\sigma = \frac{1}{2\hbar\omega_{\text{ph}}}(\sum_{\mathbf{q}} |M_{L,\mathbf{q}} \pm M_{R,\mathbf{q}}|^2)^{1/2}$ , and the upper (lower) sign corresponding to  $S(A)$ -phonons.

The mode functions for  $S$ - and  $A$ -phonons are depicted in Fig. 1(b) along a line through the centers of the quantum dots. Owing to the flat LO dispersion relation, the phonons do not diffuse and act as a cavity including the DQD.  $A$ -phonons play a crucial role for phonon-assisted tunneling and phonon lasing, as discussed below, whereas  $S$ -phonons do not since it couples to the *total* number of electrons in the DQD,  $n_L + n_R$ . Both phonons are relevant to the Franck-Condon effect, i.e., lattice distortions accompanied by electron transport between the DQD and external leads.

Our Hamiltonian is applicable to DQDs fabricated in a semiconductor substrate, where  $\hbar\omega_{\text{ph}} = 36$  meV and  $\lambda_{S(A)} \sim 0.1 - 0.01$  for  $R \sim 10 - 100$  nm in GaAs. It also describes a DQD in a suspended CNT when an electron couples to a vibron, longitudinal stretching mode with  $\hbar\omega_{\text{ph}} \sim 1$  meV,  $\lambda_A \gtrsim 1$ , and  $\lambda_S \simeq 0$  in experimental situations [11, 12].

We now consider the DQD as electronically pumped and thus connected to external leads in series. Under a large bias, an electron tunnels into dot  $L$  from the left lead with tunneling rate  $\Gamma_L$  and tunnels out from dot  $R$  to the right lead with  $\Gamma_R$  [16]. We describe the dynamics of the DQD-phonon density matrix  $\rho$  using a Markovian master equation

$$\dot{\rho} = -i[H, \rho] + \mathcal{L}_e \rho + \mathcal{L}_{\text{ph}} \rho, \quad (4)$$

where  $\mathcal{L}_e \rho = (\Gamma_L \mathcal{D}[d_L^\dagger] + \Gamma_R \mathcal{D}[d_R])\rho$  and  $\mathcal{L}_{\text{ph}} \rho = \Gamma_{\text{ph}} \sum_{\sigma=S,A} \mathcal{D}[a_\sigma] \rho$ , with  $\mathcal{D}[A]\rho = A\rho A^\dagger - \frac{1}{2}\{\rho, A^\dagger A\}$  being a Lindblad dissipator and  $\Gamma_{\text{ph}}$  the phonon escape rate [17].

In the following, we adopt the Born-Markov-Secular approximation to Eq. (4) by diagonalizing the Hamiltonian  $H$  and setting up the corresponding rate equation in the energy eigenbasis,

$$\dot{P}_i = \sum_j L_{ij} P_j \quad (5)$$

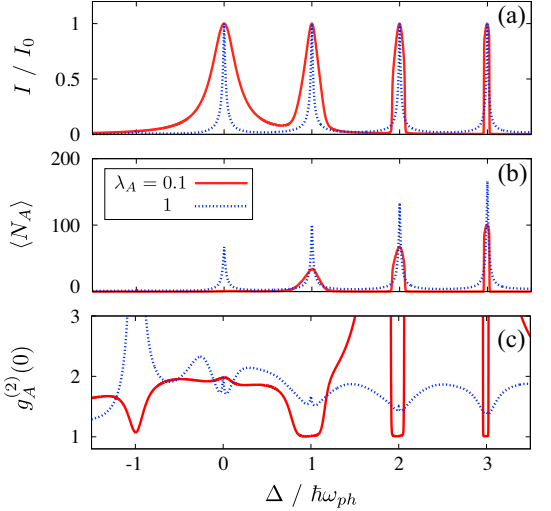


FIG. 2. (color online). (a) Electric current through the DQD, (b)  $A$ -phonon number  $\langle N_A \rangle$ , and (c) its autocorrelation function  $g_A^{(2)}(0)$ , as a function of level spacing  $\Delta$  in the DQD. The dimensionless electron-phonon couplings are  $\lambda_A = 0.1$  (solid lines) or 1 (dotted lines), and  $\lambda_S = 0$ .  $I_0 = e\Gamma_R/(2+\alpha)$  is the current at  $\Delta = 0$  in the absence of electron-phonon coupling.  $\Gamma_L = \Gamma_R = 100 \Gamma_{\text{ph}}$  and  $V_C = 0.1 \hbar\omega_{\text{ph}}$ .

for the probabilities  $P_i$  to find the system in an eigenstate  $|i\rangle$ , with  $L_{ij} = \langle i|[(\mathcal{L}_e + \mathcal{L}_{\text{ph}})|j\rangle\langle j|]i\rangle$ . The solution of Eq. (5) with  $\dot{P}_i = 0$  determines the steady state properties.

*Numerical results.*— We first discuss our numerical results in the case of  $\Gamma_{L,R} \gg \Gamma_{\text{ph}}$ . We consider  $A$ -phonons and disregard  $S$ -phonons ( $\lambda_S = 0$ ). Figure 2(a) shows the current  $I$  through the DQD as a function of level spacing  $\Delta$ , with  $\lambda_A = 0.1$  and 1. Beside the main peak at  $\Delta = 0$ , we observe subpeaks at  $\Delta \simeq \nu\hbar\omega_{\text{ph}}$  ( $\nu = 1, 2, 3, \dots$ ) due to the phonon-assisted tunneling. At the  $\nu$ th subpeak, electron transport through the DQD is accompanied by the emission of  $\nu$  phonons. As a result, the phonon number is markedly enhanced at the subpeaks, as shown in Fig. 2(b), in both cases of  $\lambda_A = 0.1$  and 1. As we will show now, however, the physics is very different for the two cases.

For  $\lambda_S = 0.1$  and  $\Delta \simeq \nu\hbar\omega_{\text{ph}}$ , the electronic state  $|L\rangle$  with  $n$  phonons is coherently coupled to  $|R\rangle$  with  $(n + \nu)$  phonons [18], similarly to a microlaser two-level system in a photon cavity, if the lattice distortion can be neglected. To examine the amplification of  $A$ -phonons, we calculate the phonon autocorrelation function,  $g_A^{(2)}(\tau) \equiv \langle : N_A(0)N_A(\tau) :\rangle / \langle N_A \rangle^2$ , which is the probability of phonon emission at time  $\tau$  on the condition that a phonon is emitted at time 0 [19, 20]. A value of  $g_A^{(2)}(0) = 1$  indicates a *Poissonian* distribution of phonons which is a criterion of phonon lasing. We thus find phonon lasing at the current subpeaks in Fig. 2(c). We mention that these are not qualitatively changed in the presence of a finite coupling  $\lambda_S$  to  $S$ -phonons.

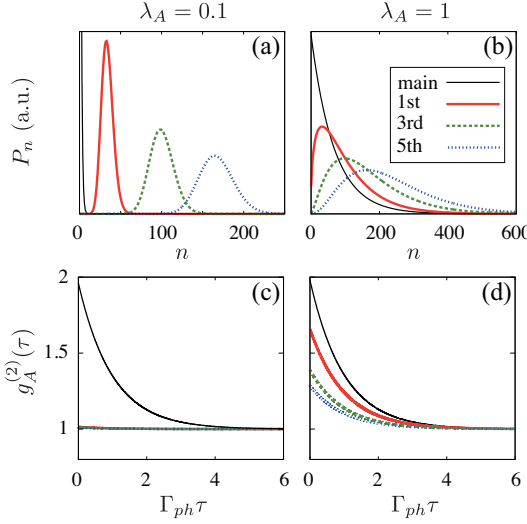


FIG. 3. (color online). (a), (b) The number distribution of  $A$ -phonons and (c), (d) its autocorrelation function  $g_A^{(2)}(\tau)$  at the current main peak and subpeaks ( $\nu = 1, 3, 5$ ). The dimensionless electron-phonon couplings are  $\lambda_A = 0.1$  [1] in panels (a) and (c) [(b) and (d)] and  $\lambda_S = 0$ . Note that three lines for the current subpeaks are almost overlapped in panel (c).  $\Gamma_L = \Gamma_R = 100 \Gamma_{\text{ph}}$  and  $V_C = 0.1 \hbar\omega_{\text{ph}}$ .

When  $\lambda_A = 1$ , the strength of the electron-phonon interaction is comparable to the phonon energy. In this case, the lattice distortion by the Franck-Condon effect seriously disturbs the above-mentioned coherent coupling between an electron and phonons in the DQD and, as a result, suppresses the phonon lasing. Indeed,  $g_A^{(2)}(0) > 1$  at the current subpeaks.

To compare the two situations in detail, we show the number distribution of  $A$ -phonons in Figs. 3(a) and (b) at the current main peak and subpeaks. In the case of  $\lambda_A = 0.1$ , a Poisson-like distribution emerges at the subpeaks, whereas a Bose distribution with temperature  $T^*$

is seen at the main peak.  $T^*$  is determined from the number of phonons  $\langle N_A \rangle$  in the stationary state. When  $\lambda_A = 1$ , on the other hand, the distribution shows an intermediate shape between a Poissonian and a Bose distributions at the subpeaks and a Bose distribution at the main peak. In Figs. 3(c) and (d), we plot the autocorrelation function  $g_A^{(2)}(\tau)$  of  $A$ -phonons. In the case of  $\lambda_A = 0.1$ ,  $g_{\text{ph}}^{(2)}(\tau) \simeq 1$ , regardless of the time delay  $\tau$ , supports the phonon lasing at the current subpeaks. At the main peak,  $g_{\text{ph}}^{(2)}(\tau) \simeq 1 + e^{-\Gamma_{\text{ph}}\tau}$ , which is a character of thermal phonons with effective temperature  $T^*$ . When  $\lambda_A = 1$ , we find an intermediate behavior,  $g_{\text{ph}}^{(2)}(\tau) \simeq 1 + \delta_\nu e^{-\Gamma_{\text{ph}}\tau}$  ( $0 < \delta_\nu < 1$ ), at the  $\nu$ th subpeak. This indicates that the phonons are partly thermalized by the Franck-Condon effect. For larger  $\nu$ , the distribution is closer to the Poissonian with smaller  $\delta_\nu$ .

*Analytical results.*— To elucidate the competition between the phonon lasing and the thermalization by the Franck-Condon effect, we analyze the rate equation in Eq. (5) at the current peaks. We introduce polaron states  $|L(R), n\rangle$  for an electron in dot  $L$  ( $R$ ) and  $n$  phonons with lattice distortion:

$$|L(R), n\rangle = |L(R)\rangle \otimes \mathcal{T}^{(\dagger)}|n\rangle_A, \quad \mathcal{T} = e^{-\lambda_A(a_A^\dagger - a_A)}, \quad (6)$$

where  $\mathcal{T}$  and  $\mathcal{T}^\dagger$  describe the shift of equilibrium position of the lattice when an electron stays in dot  $L$  and  $R$ , respectively. Note that the lattice distortion produces  $\lambda_A^2$  extra phonons:  $\langle \alpha, n | N_A | \alpha, n \rangle = n + \lambda_A^2$ . When  $\Delta \simeq \nu \hbar\omega_{\text{ph}}$ , the eigenstates of Hamiltonian  $H$  are given by the zero-electron states  $|0, n\rangle = |0\rangle \otimes |n\rangle_A$ , bonding and anti-bonding states between the polarons,

$$|\pm, n\rangle = \frac{1}{\sqrt{2}}(|L, n\rangle \pm |R, n + \nu\rangle) \quad (7)$$

( $n = 0, 1, 2, \dots$ ) and polarons localized in dot  $R$ ,  $|R, n\rangle$  ( $n = 0, 1, 2, \dots, \nu - 1$ ), in a good approximation, provided that  $V_C \ll \hbar\omega_{\text{ph}}$ . The rate equations for these states are

$$\dot{P}_{0,n} = -\Gamma_L P_{0,n} + \sum_{m=0}^{\infty} \frac{\Gamma_R}{2} |A\langle n | \mathcal{T}^\dagger | m + \nu \rangle_A|^2 P_{\text{mol},m} + \sum_{m=0}^{\nu-1} \Gamma_R |A\langle n | \mathcal{T}^\dagger | m \rangle_A|^2 P_{R,m} + \Gamma_{\text{ph}} [(n+1)P_{0,n+1} - nP_{0,n}], \quad (8)$$

$$\dot{P}_{\text{mol},n} = -\frac{\Gamma_R}{2} P_{\text{mol},n} + \sum_{m=0}^{\infty} \Gamma_L |A\langle n | \mathcal{T} | m \rangle_A|^2 P_{0,m} + \Gamma_{\text{ph}} \left[ \left( n + 1 + \frac{\nu}{2} \right) P_{\text{mol},n+1} - \left( n + \frac{\nu}{2} \right) P_{\text{mol},n} \right], \quad (9)$$

where  $P_{\text{mol},n} = P_{+,n} + P_{-,n}$  ( $n = 0, 1, 2, \dots$ ), and

$$\dot{P}_{R,n} = -\Gamma_R P_{R,n} + \Gamma_{\text{ph}} [(n+1)P_{R,n+1} - nP_{R,n}], \quad (10)$$

with  $P_{R,\nu} = P_{\text{mol},0}/2$  ( $n = 0, 1, 2, \dots, \nu - 1$ ). These equations yield the current  $I$  and the electron number in the

DQD  $\langle n_e \rangle \equiv \langle n_L + n_R \rangle$  in terms of the number of polarons localized in dot  $R$ ,  $\langle \tilde{n}_R \rangle = \sum_{n=0}^{\nu-1} P_{R,n}$  as

$$I = e\Gamma_R \frac{1 + \langle \tilde{n}_R \rangle}{2 + \alpha}, \quad \langle n_e \rangle = \frac{2 - \alpha \langle \tilde{n}_R \rangle}{2 + \alpha} \quad (11)$$

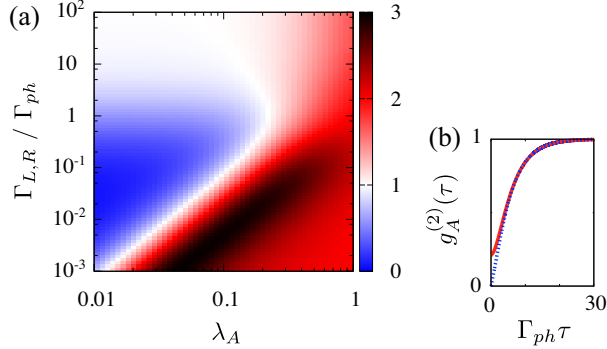


FIG. 4. (color online). (a) Color-scale plot of autocorrelation function of  $A$ -phonons,  $g_A^{(2)}(0)$ , at the first subpeak of current in a plane of electron-phonon coupling  $\lambda_A$  and  $\Gamma_{L,R}/\Gamma_{\text{ph}}$ .  $\Gamma_L = \Gamma_R \equiv \Gamma_{L,R}$ ,  $\lambda_S = 0$ , and  $V_C = 0.1 \hbar\omega_{\text{ph}}$ . (b)  $g_A^{(2)}(\tau)$  at  $\lambda_A = 0.05$  and  $\Gamma_{L,R} = 0.1 \Gamma_{\text{ph}}$  (solid line). Dotted line: electric current autocorrelation function  $g_{\text{current}}^{(2)}(\tau)$ .

with  $\alpha \equiv \Gamma_R/\Gamma_L$ . The number of  $A$ -phonons is given by

$$\langle N_A \rangle = (\nu + 2\lambda_A^2) \frac{I}{e\Gamma_{\text{ph}}} + \lambda_A^2 \langle n_e \rangle. \quad (12)$$

The first two terms in Eq. (12) indicate the emission of  $\nu$  phonons by the phonon-assisted tunneling (from dot  $L$  to dot  $R$ ) and creation of  $2\lambda_A^2$  phonons by the lattice distortion (with two tunnelings between the DQD and leads) per transfer of a single electron through the DQD. The last term describes the average number of polarons  $\langle n_e \rangle$  in the stationary state.

When  $\Gamma_{L,R} \gg \Gamma_{\text{ph}}$ , we find  $I = I_0 + \mathcal{O}(\Gamma_{\text{ph}}/\Gamma_{L,R})$ , where  $I_0 = e\Gamma_R/(2 + \alpha)$  is the current at the main peak in the absence of electron-phonon interaction. The calculation (Supplemental Material) yields

$$g_A^{(2)}(0) = \frac{\nu + 4\lambda_A^2}{\nu + 2\lambda_A^2} + \mathcal{O}(\Gamma_{\text{ph}}/\Gamma_{L,R}), \quad (13)$$

which explains the numerical results in Fig. 2(c) at the current subpeaks. This formula indicates  $g_A^{(2)}(0) \simeq 1$  (phonon lasing) for  $\lambda_A^2 \ll \nu$  and  $g_A^{(2)}(0) \simeq 2$  (thermalized phonons by the lattice distortion) for  $\lambda_A^2 \gg \nu$ . In the latter case, the phonons follow the Bose distribution with  $T^*$  to deduce  $\langle N_A \rangle$  in Eq. (12).

*Phonon anti-bunching.*— So far we have only discussed the case of  $\Gamma_{L,R} \gg \Gamma_{\text{ph}}$  where the escape rate of phonons is so small that the phonons surrounding the DQD work as a cavity. If the tunnel coupling is tuned to be  $\Gamma_{L,R} \lesssim \Gamma_{\text{ph}}$ , we observe another phenomenon, i.e., anti-bunching of LO phonons [21]. Figure 4(a) presents a color-scale plot of  $g_A^{(2)}(0)$  at the first current subpeak in the  $\lambda_A$ – $(\Gamma_{L,R}/\Gamma_{\text{ph}})$  plane for  $\Gamma_L = \Gamma_R \equiv \Gamma_{L,R}$  and  $\lambda_S = 0$ . At  $\lambda_A = 0.05$  and  $\Gamma_{L,R}/\Gamma_{\text{ph}} = 0.1$ , for example,  $g_A^{(2)}(0) \ll 1$ , representing a strong anti-bunching of phonons. This is because the phonon emission is regularized by the

electron transport through the DQD. In Fig. 4(b), we plot the autocorrelation function of the electronic current,  $g_{\text{current}}^{(2)}(\tau) = \langle : n_R(0)n_R(\tau) : \rangle / \langle n_R \rangle^2$ , where  $n_R$  is the electron number in dot  $R$ . It fulfills  $g_{\text{current}}^{(2)}(0) = 0$  since dot  $R$  is empty just after the electron tunnels out (anti-bunching of electron transport) [20]. Remarkably,  $g_A^{(2)}(\tau)$  almost coincides with  $g_{\text{current}}^{(2)}(\tau)$ . Again at very strong couplings  $\lambda_A \gtrsim 1$ , neither phonon anti-bunching nor phonon lasing can be observed because of an effective phonon thermalization due to the Franck-Condon effect.

In our calculations, we have neglected the  $S$ -phonon coupling which, however, does not influence the phenomena for  $\lambda_A \lesssim 0.1$  as we have checked. We have also disregarded the coupling to acoustic phonons. At small wavenumbers  $|\mathbf{q}| \lesssim 1/R$ , their energy is much smaller than the energy of LO phonons  $\hbar\omega_{\text{ph}}$  [7] and they should therefore play a minor role in the present context.

Finally, we discuss possible experimental realizations to observe LO phonon lasing in semiconductor-based DQDs. LO-phonon-assisted transport has been observed for level spacings  $\Delta$  tuned to  $\hbar\omega_{\text{ph}}$  and  $2\hbar\omega_{\text{ph}}$  in recent experiments [15]. An LO phonon around the  $\Gamma$  point decays into an LO phonon and a TA phonon around the L point (daughter phonons), which are not coupled to the DQD. With a decay rate  $\Gamma_{\text{ph}} \sim 10^{11}$  Hz in bulk GaAs [8], the condition  $\Gamma_{L,R} \gg \Gamma_{\text{ph}}$  might be hard to realize. However, it should be possible to significantly tune  $\Gamma_{\text{ph}}$  via low temperatures and an appropriate DQD design. If the phonon lasing is realized, we expect the creation of a large amount of daughter phonons escaping from the DQD surrounding. These phonons can then be detected by the transport through another DQD fabricated nearby [22, 23]. Alternatively, the modulation of the dielectric constant by the phonons could be observed by near-field spectroscopy [24].

The authors acknowledge fruitful discussion with K. Ono, S. Amaha, Y. Kayanuma, K. Saito, C. Pöltl, T. Yokoyama, and A. Yamada. This work was partially supported by KAKENHI (23104724), Institutional Program for Young Researcher Oversea Visits and International Training Program from the Japan Society for the Promotion of Science, Graduate School Doctoral Student Aid Program from Keio University, and the German DFG via SFB 910 and project BR 1528/8-1.

\* [rakuyama@rk.phys.keio.ac.jp](mailto:rakuyama@rk.phys.keio.ac.jp)

- [1] O. Astafiev, K. Inomata, A. O. Niskanen, T. Yamamoto, Y. A. Pashkin, Y. Nakamura, and J. S. Tsai, *Nature* **449**, 588 (2007).
- [2] D. A. Rodrigues, J. Imbers, and A. D. Armour, *Phys. Rev. Lett.* **98**, 067204 (2007).
- [3] S. André, V. Brosco, A. Shnirman, and G. Schön, *Phys. Rev. A* **79**, 053848 (2009).
- [4] J. McKeever, A. Boca, A. D. Boozer, J. R. Buck, and H.

J. Kimble, *Nature* **425**, 268 (2003).

[5] T. Fujisawa, T. H. Oosterkamp, W. G. van der Wiel, B. W. Broer, R. Aguado, S. Tarucha, and L. P. Kouwenhoven, *Science* **282**, 932 (1998).

[6] T. Brandes and B. Kramer, *Phys. Rev. Lett.* **83**, 3021 (1999).

[7] P. Roulleau, S. Baer, T. Choi, F. Molitor, J. Güttinger, T. Müller, S. Dröscher, K. Ensslin, and T. Ihn, *Nat. Commun.* **2**, 239 (2011).

[8] F. Vallée, *Phys. Rev. B* **49**, 2460 (1994).

[9] P. Gartner, *Phys. Rev. A* **84**, 053804 (2011).

[10] J. Koch and F. von Oppen, *Phys. Rev. Lett.* **94**, 206804 (2005).

[11] S. Sapmaz, P. Jarillo-Herrero, Y. M. Blanter, C. Dekker, and H. S. J. van der Zant, *Phys. Rev. Lett.* **96**, 026801 (2006).

[12] R. Leturcq, C. Stampfer, K. Inderbitzin, L. Durrer, C. Hierold, E. Mariani, M. G. Schultz, F. von Oppen, and K. Ensslin, *Nat. Phys.* **5**, 327 (2009).

[13] P.-Q. Jin, M. Marthaler, J. H. Cole, A. Shnirman, and G. Schön, arXiv:1205.0436 (2012).

[14] C. Gnodtke, G. Kießlich, E. Schöll, and A. Wacker, *Phys. Rev. B* **73**, 115338 (2006).

[15] S. Amaha and K. Ono, private communications.

[16] When the bias voltage is not large enough, the current is suppressed by the Franck-Condon blockade. Here, we assume a large bias to avoid the blockade.

[17] T. Brandes, N. Lambert, *Phys. Rev. B* **67**, 125323 (2003).

[18] S. Hameau, Y. Guldner, O. Verzelen, R. Ferreira, G. Bastard, J. Zeman, A. Lemaître, and J. M. Gérard, *Phys. Rev. Lett.* **83**, 4152 (1999).

[19] M. O. Scully and M. S. Zubairy, *Quantum Optics* (Cambridge University Press, Cambridge, 1997).

[20] C. Emery, C. Pöltl, A. Carmele, J. Kabuss, A. Knorr, and T. Brandes, *Phys. Rev. B* **85**, 165417 (2012).

[21] N. Lambert and F. Nori, *Phys. Rev. B* **78**, 214302 (2008).

[22] U. Gasser, S. Gustavsson, B. Küng, K. Ensslin, T. Ihn, D. C. Driscoll, and A. C. Gossard, *Phys. Rev. B* **79**, 035303 (2009).

[23] D. Harbusch, D. Taubert, H. P. Tranitz, W. Wegscheider, and S. Ludwig, *Phys. Rev. Lett.* **104**, 196801 (2010).

[24] J. Cunningham, M. Byrne, P. Upadhyay, M. Lachab, E. H. Linfield, and A. G. Davies, *Appl. Phys. Lett.* **92**, 032903 (2008).

## Supplementary Material for “Optical Phonon Lasing in Semiconductor Double Quantum Dots”

Rin Okuyama<sup>1</sup>, Mikio Eto<sup>1</sup>, and Tobias Brandes<sup>2</sup>

<sup>1</sup>Faculty of Science and Technology, Keio University, Yokohama 223-8522, Japan

<sup>2</sup>Institut für Theoretische Physik, Technische Universität Berlin, D-10623 Berlin, Germany

In this supplementary material, we derive analytical expressions for the current  $I$ , number of phonons  $\langle N_A \rangle$ , and autocorrelation function of phonons  $g_A^{(2)}(0)$  at the current subpeaks in Eqs. (11)–(13) in the main material. When  $\Delta \simeq \nu \hbar \omega_{\text{ph}}$ , the energy eigenstates are given by the zero-electron states  $|0, n\rangle = |0\rangle \otimes |n\rangle_A$ , bonding and anti-bonding states between polarons  $|\pm, n\rangle = \frac{1}{\sqrt{2}} (|L, n\rangle \pm |R, n + \nu\rangle)$ , and polarons localized in dot  $R$ ,  $|R, n\rangle$  ( $n = 0, 1, 2, \dots, \nu-1$ ), in a good approximation for  $V_C \ll \hbar \omega_{\text{ph}}$ , as mentioned in the main material. We have introduced polaron states  $|L(R), n\rangle = |L(R)\rangle \otimes \mathcal{T}^{(\dagger)}|n\rangle_A$ , with  $\mathcal{T} = e^{-\lambda_A(a_A^\dagger - a_A)}$ . The density matrix is given by

$$\rho = \sum_{n=0}^{\infty} P_{0,n} |0, n\rangle \langle 0, n| + \sum_{\tau=\pm} \sum_{n=0}^{\infty} P_{\tau,n} |\tau, n\rangle \langle \tau, n| + \sum_{n=0}^{\nu-1} P_{R,n} |R, n\rangle \langle R, n| \quad (14)$$

in the Born-Markov-Secular approximation. We define occupation number operators for zero-electron states, bonding and anti-bonding states between the polarons, and polarons localized in dot  $R$  as

$$n_0 = \sum_{n=0}^{\infty} |0, n\rangle \langle 0, n| = |0\rangle \langle 0|, \quad n_{\text{mol}} = \sum_{\tau=\pm} \sum_{n=0}^{\infty} |\tau, n\rangle \langle \tau, n|, \quad \tilde{n}_R = \sum_{n=0}^{\nu-1} |R, n\rangle \langle R, n|, \quad (15)$$

respectively. The relation of  $n_0 + n_{\text{mol}} + \tilde{n}_R = 1$  holds. The electron number in the DQD is given by  $n_e = n_{\text{mol}} + \tilde{n}_R = 1 - n_0$ . The expectation values of the occupation numbers are

$$\langle n_0 \rangle = \sum_{n=0}^{\infty} P_{0,n}, \quad \langle n_{\text{mol}} \rangle = \sum_{n=0}^{\infty} P_{\text{mol},n}, \quad \langle \tilde{n}_R \rangle = \sum_{n=0}^{\nu-1} P_{R,n}. \quad (16)$$

In the stationary state, the rate equations in Eqs. (8)–(10) in the main material yield

$$0 = -\Gamma_L P_{0,n} + \sum_{m=0}^{\infty} \frac{\Gamma_R}{2} |{}_A\langle n|\mathcal{T}^\dagger|m+\nu\rangle_A|^2 P_{\text{mol},m} + \sum_{m=0}^{\nu-1} \Gamma_R |{}_A\langle n|\mathcal{T}^\dagger|m\rangle_A|^2 P_{R,m} + \Gamma_{\text{ph}} [(n+1)P_{0,n+1} - nP_{0,n}], \quad (17)$$

$$0 = -\frac{\Gamma_R}{2} P_{\text{mol},n} + \sum_{m=0}^{\infty} \Gamma_L |{}_A\langle n|\mathcal{T}|m\rangle_A|^2 P_{0,m} + \Gamma_{\text{ph}} \left[ \left( n+1 + \frac{\nu}{2} \right) P_{\text{mol},n+1} - \left( n + \frac{\nu}{2} \right) P_{\text{mol},n} \right], \quad (18)$$

with  $P_{\text{mol},n} = P_{+,n} + P_{-,n}$  ( $n = 0, 1, 2, \dots$ ), and

$$0 = -\Gamma_R P_{R,n} + \Gamma_{\text{ph}} [(n+1)P_{R,n+1} - nP_{R,n}], \quad (19)$$

with  $P_{R,\nu} = P_{\text{mol},0}/2$  ( $n = 0, 1, 2, \dots, \nu - 1$ ).

## CURRENT AND ELECTRON NUMBER

First, we express the current  $I = e\Gamma_L \langle n_0 \rangle$  in the stationary state. For the purpose, we sum up both sides of Eq. (17) over  $n$ . Using

$$\sum_{n=0}^{\infty} |{}_A\langle n|\mathcal{T}^\dagger|m\rangle_A|^2 = {}_A\langle m|\mathcal{T} \left( \sum_n |n\rangle_{AA}\langle n| \right) \mathcal{T}^\dagger|m\rangle_A = 1, \quad (20)$$

we obtain

$$0 = -\Gamma_L \langle n_0 \rangle + \frac{\Gamma_R}{2} \langle n_{\text{mol}} \rangle + \Gamma_R \langle \tilde{n}_R \rangle. \quad (21)$$

With  $\langle n_0 \rangle + \langle n_{\text{mol}} \rangle + \langle \tilde{n}_R \rangle = 1$ , we derive

$$\langle n_0 \rangle = \frac{\alpha}{2+\alpha} (1 + \langle \tilde{n}_R \rangle), \quad \langle n_{\text{mol}} \rangle = \frac{2}{2+\alpha} [1 - (1+\alpha)\langle \tilde{n}_R \rangle], \quad (22)$$

with  $\alpha = \Gamma_R/\Gamma_L$ . These equations result in Eq. (11) in the main material:

$$I = e\Gamma_R \frac{1 + \langle \tilde{n}_R \rangle}{2 + \alpha}, \quad \langle n_e \rangle = \frac{2 - \alpha \langle \tilde{n}_R \rangle}{2 + \alpha}. \quad (23)$$

The summation of Eq. (19) over  $n$  yields

$$\langle \tilde{n}_R \rangle = \frac{\nu \Gamma_{\text{ph}}}{2 \Gamma_R} P_{\text{mol},0}. \quad (24)$$

## PHONON NUMBER

Next, we derive the phonon number which is

$$\langle N_A \rangle = \sum_{n=0}^{\infty} P_{0,n} \langle 0, n | N_A | 0, n \rangle + \sum_{\tau=\pm} \sum_{n=0}^{\infty} P_{\tau,n} \langle \tau, n | N_A | \tau, n \rangle + \sum_{n=0}^{\nu-1} P_{R,\nu} \langle R, n | N_A | R, n \rangle \quad (25)$$

$$= \sum_{n=0}^{\infty} n P_{0,n} + \sum_{n=0}^{\infty} \left( n + \frac{\nu}{2} + \lambda_A^2 \right) P_{\text{mol},n} + \sum_{n=0}^{\nu-1} (n + \lambda_A^2) P_{R,n} \quad (26)$$

$$\equiv \langle N_A n_0 \rangle + \langle N_A n_{\text{mol}} \rangle + \langle N_A \tilde{n}_R \rangle. \quad (27)$$

We have used

$$\mathcal{T}^\dagger N_A \mathcal{T} = (\mathcal{T}^\dagger a_A^\dagger \mathcal{T})(\mathcal{T}^\dagger a_A \mathcal{T}) = (a_A^\dagger - \lambda_A)(a_A - \lambda_A). \quad (28)$$

We multiply both sides of Eqs. (17)–(19) by  $n$  and sum up over  $n$ :

$$0 = -(\Gamma_L + \Gamma_{\text{ph}})\langle N_A n_0 \rangle + \frac{\Gamma_R}{2}\langle N_A n_{\text{mol}} \rangle + \Gamma_R\langle N_A \tilde{n}_R \rangle + \frac{\nu \Gamma_R}{4}\langle n_{\text{mol}} \rangle, \quad (29)$$

$$0 = \Gamma_L\langle N_A n_0 \rangle - \left( \frac{\Gamma_R}{2} + \Gamma_{\text{ph}} \right) \langle N_A n_{\text{mol}} \rangle + \lambda_A^2 \Gamma_L \langle n_0 \rangle + \left( \frac{\nu + 2\lambda_A^2}{4} \Gamma_R + \lambda_A^2 \Gamma_{\text{ph}} \right) \langle n_{\text{mol}} \rangle + \Gamma_R \langle \tilde{n}_R \rangle, \quad (30)$$

$$0 = -(\Gamma_R + \Gamma_{\text{ph}})\langle N_A \tilde{n}_R \rangle + [(\nu - 1 + \lambda_A^2)\Gamma_R + \lambda_A^2 \Gamma_{\text{ph}}] \langle \tilde{n}_R \rangle. \quad (31)$$

Here, we have used

$$\sum_{n=0}^{\infty} n \left| {}_A \langle n | \mathcal{T}^\dagger | m \rangle_A \right|^2 = {}_A \langle m | \mathcal{T} N_A \left( \sum_n |n\rangle_{AA} \langle n| \right) \mathcal{T}^\dagger | m \rangle_A = \sum_m {}_A \langle m | \mathcal{T} N_A \mathcal{T}^\dagger | m \rangle_A. \quad (32)$$

From Eqs. (29)–(31), we obtain Eq. (12) in the main material:

$$\langle N_A \rangle = (\nu + 2\lambda_A^2) \frac{I}{e\Gamma_{\text{ph}}} + \lambda_A^2 \langle n_e \rangle. \quad (33)$$

## PHONON AUTOCORRELATION FUNCTION

Finally, we derive the phonon autocorrelation function at zero time delay,

$$g_A^{(2)}(0) = \frac{\langle : N_A^2 : \rangle}{\langle N_A \rangle^2} = \frac{\langle N_A^2 \rangle - \langle N_A \rangle}{\langle N_A \rangle^2}, \quad (34)$$

where

$$\langle N_A^2 \rangle = \sum_{n=0}^{\infty} P_{0,n} \langle 0, n | N_A^2 | 0, n \rangle + \sum_{\tau=\pm} \sum_{n=0}^{\infty} P_{\tau,n} \langle \tau, n | N_A^2 | \tau, n \rangle + \sum_{n=0}^{\nu-1} P_{R,\nu} \langle R, n | N_A^2 | R, n \rangle \quad (35)$$

$$= \sum_{n=0}^{\infty} n^2 P_{0,n} + \sum_{n=0}^{\infty} \left[ n^2 + \lambda_A^2 (4n + 1 + \lambda_A^2) + \nu \left( n + \frac{\nu}{2} + 2\lambda_A^2 \right) \right] P_{\text{mol},n} + \sum_{n=0}^{\nu-1} [n^2 + \lambda_A^2 (4n + 1 + \lambda_A^2)] P_{R,n} \quad (36)$$

$$\equiv \langle N_A^2 n_0 \rangle + \langle N_A^2 n_{\text{mol}} \rangle + \langle N_A^2 \tilde{n}_R \rangle. \quad (37)$$

We multiply both sides of Eqs. (17)–(19) by  $n^2$  and sum up over  $n$ . A similar technique to the last section leads to

$$0 = -(\Gamma_L + 2\Gamma_{\text{ph}})\langle N_A^2 n_0 \rangle + \frac{\Gamma_R}{2}\langle N_A^2 n_{\text{mol}} \rangle + \Gamma_R\langle N_A^2 \tilde{n}_R \rangle + \Gamma_{\text{ph}}\langle N_A n_0 \rangle + \frac{\nu \Gamma_R}{2}\langle N_A n_{\text{mol}} \rangle + \frac{\nu \lambda_A^2 \Gamma_R}{2}\langle n_{\text{mol}} \rangle, \quad (38)$$

$$0 = \Gamma_L\langle N_A^2 n_0 \rangle - \left( \frac{\Gamma_R}{2} + 2\Gamma_{\text{ph}} \right) \langle N_A^2 n_{\text{mol}} \rangle + 4\lambda_A^2 \Gamma_L \langle N_A n_0 \rangle + \left[ \frac{\nu + 4\lambda_A^2}{2} \Gamma_R + (\nu + 1 + 8\lambda_A^2) \Gamma_{\text{ph}} \right] \langle N_A n_{\text{mol}} \rangle + \lambda_A^2 (1 + \lambda_A^2) \Gamma_L \langle n_0 \rangle + \lambda_A^2 \left[ \frac{1 - \nu - 3\lambda_A^2}{2} \Gamma_R + (1 - \nu - 6\lambda_A^2) \Gamma_{\text{ph}} \right] \langle n_{\text{mol}} \rangle - \Gamma_R \langle \tilde{n}_R \rangle, \quad (39)$$

$$0 = -(\Gamma_R + 2\Gamma_{\text{ph}})\langle N_A^2 \tilde{n}_R \rangle + [4\lambda_A^2 \Gamma_R + (1 + 8\lambda_A^2) \Gamma_{\text{ph}}] \langle N_A \tilde{n}_R \rangle + \{ [(\nu - 1)^2 + \lambda_A^2 (1 - 3\lambda_A^2)] \Gamma_R + \lambda_A^2 (1 - 6\lambda_A^2) \Gamma_{\text{ph}} \} \langle \tilde{n}_R \rangle. \quad (40)$$

From Eqs. (38)–(40), we find

$$\begin{aligned} \langle N_A^2 \rangle - \langle N_A \rangle &= 2\lambda_A^2 \frac{\Gamma_L}{\Gamma_{\text{ph}}} \langle N_A n_0 \rangle + \left( \frac{\nu + 2\lambda_A^2}{2} \frac{\Gamma_R}{\Gamma_{\text{ph}}} + \frac{\nu + 4\lambda_A^2}{2} \right) \langle N_A n_{\text{mol}} \rangle + 2\lambda_A^2 \left( \frac{\Gamma_R}{\Gamma_{\text{ph}}} + 2 \right) \langle N_A \tilde{n}_R \rangle \\ &\quad - \frac{\nu + 2\lambda_A^4}{2} \frac{\Gamma_L}{\Gamma_{\text{ph}}} \langle n_0 \rangle - \frac{\lambda_A^2 (\nu + 6\lambda_A^2)}{2} \langle n_{\text{mol}} \rangle - \left[ \frac{\nu (2 - \nu)}{2} \frac{\Gamma_R}{\Gamma_{\text{ph}}} + 3\lambda_A^2 \right] \langle \tilde{n}_R \rangle. \end{aligned} \quad (41)$$

Now we evaluate  $g_A^{(2)}(0)$  in the case of  $\Gamma_{L,R} \gg \Gamma_{\text{ph}}$ . In this case,  $\langle \tilde{n}_R \rangle = \mathcal{O}(\Gamma_{\text{ph}}/\Gamma_{L,R})$  from Eq. (24). Then

$$I = \frac{e\Gamma_R}{2 + \alpha} + \mathcal{O}(\Gamma_{\text{ph}}/\Gamma_{L,R}) \quad (42)$$

and

$$\langle N_A \rangle = \frac{\nu + 2\lambda_A^2}{2 + \alpha} \frac{\Gamma_R}{\Gamma_{\text{ph}}} + \mathcal{O}(1). \quad (43)$$

Equations (29) and (31) yield

$$2\langle N_A n_0 \rangle = \alpha \langle N_A n_{\text{mol}} \rangle + \mathcal{O}(1), \quad \langle N_A \tilde{n}_R \rangle = \mathcal{O}(\Gamma_{\text{ph}}/\Gamma_{L,R}). \quad (44)$$

Using  $\langle N_A \rangle = \langle N_A n_0 \rangle + \langle N_A n_{\text{mol}} \rangle + \langle N_A \tilde{n}_R \rangle$ , we have

$$\langle N_A n_0 \rangle = (\nu + 2\lambda_A^2) \frac{\alpha}{(2 + \alpha)^2} \frac{\Gamma_R}{\Gamma_{\text{ph}}} + \mathcal{O}(1), \quad \langle N_A n_{\text{mol}} \rangle = (\nu + 2\lambda_A^2) \frac{2}{(2 + \alpha)^2} \frac{\Gamma_R}{\Gamma_{\text{ph}}} + \mathcal{O}(1). \quad (45)$$

Using these relations, we obtain Eq. (13) in the main material:

$$g_A^{(2)}(0) = \frac{\nu + 4\lambda_A^2}{\nu + 2\lambda_A} + \mathcal{O}(\Gamma_{\text{ph}}/\Gamma_{L,R}). \quad (46)$$

---